文章编号:0258-7106 (2002) 03-0270-08

金顶铅锌矿床地质-地球化学*

薛春纪[1] 陈毓川[2] 杨建民[3] 王登红[3] 杨伟光[4] 杨清标[4]

(1 长安大学成矿作用及其动力学国土资源部开放研究实验室, 长安大学地矿系, 陕西 西安 710054; 2 中国地质科学院, 北京 100037; 3 中国地质科学院矿产资源研究所, 北京 100037; 4 云南地质三大队, 云南 大理 671000)

摘 要 金顶铅锌矿床的成矿作用发生在中-新生代沉积地层当中,且矿区内没有明显出露岩浆岩,矿体为板状,产在古新统云龙组和下白垩统景星组的陆相碎屑岩中,但成矿并不受岩相地层控制,而受断裂和穹隆构造控制。铅同位素数据指示成矿金属主要来自地幔。硫同位素具有 $\delta^{34}S_{黄铁矿} > \delta^{34}S_{闪锌矿} > \delta^{34}S_{方铅矿}$ 的趋势,硫主要来自地壳。闪锌矿及有关脉石矿物(石英、天青石、方解石和硬石膏)的流体包裹体研究表明,均一温度主要在 110 ~ 150 ℃,盐度 $w(NaCl_{eq})$ 5.09 % ~ 19.63 %,成矿压力 32.5 ~ 22.6 MPa,所对应的成矿深度 0.9 ~ 1.5 km。

关键词 地层与构造控制 铅和硫同位素 均一温度 盐度 金顶矿床

中图分类号: P618.42;P618.43 **文献标识码**: A

金顶铅锌矿床 1957 年被发现,Pb-Zn 控制储量 1 500 万 t(平均品位 w_{Pb} 1.29 %, w_{Zn} 6.08 %),成矿总金属量大于 2 200 万 t❶,是目前中国最大铅-锌矿床;同时 Tl(8 167 t)、Cd(17 万 t)、Ag(1 722 t)、S(513 万 t)、Sr(147 万 t)也分别达到大型矿床规模。

金顶矿床在成因上有别于其他地区以沉积岩为主岩的 MVT、SEDEX 型及砂岩型(SST)铅锌矿床。尽管它以碎屑沉积岩为主岩,但成矿背景、矿体产状及 w_{Pb}/w_{Zn} 值等都与 SST 铅(锌)矿床不同;虽以陆相碎屑岩为主岩,又不同于以海相碳酸盐岩为主岩的 MVT 矿床;矿石的产状、微细粒组构及 w_{Pb}/w_{Zn} 值与 SEDEX 型矿床相似,但没有确切的沉积成矿事实及与之相伴的热水沉积岩,成矿背景不同于后者。金顶矿床也许是以沉积岩为主岩的铅锌矿床的一种新类型,对其研究不仅具有重要成矿学意义,而且为在其他地方寻找类似的矿床积累经验。

金顶矿床研究始于上世纪 80 年代,认为是同生沉积-后期改造层控矿床(施加辛等,1983;白嘉芬等,1985)。中国地质大学作了多方面研究,但认识分歧较大,提出“中低温非岩浆热液成矿”(高广立,1989)、“同生沉积-变形叠加成矿”(吴淦国等,1989)、“喷气(热液)沉积成矿”(赵兴元,1989)、“岩溶成矿”(胡明安,1989)等认识。90 年代以来,兰坪-思茅盆地演化深部控制因素研究指出盆地内存在幔-壳复合成矿作用(尹汉辉等,1990),矿床 REE 地球化学研究推测成矿物质主要来源于富 CO_2 的地幔流体(王京彬等,1991),提出“层控型后生矿床”观点(覃功炯等,1991),矿床铅同位素组成指示硫化物矿石铅为幔源铅(周维全等,1992;张乾,1993),并认为矿床具有“同生沉积-沉积改造-后期幔源铅叠加”的复杂形成过程(张乾,1993;叶庆同等,1992)。然而更多研究者把金顶矿床理解为陆相热水沉积成因(罗君烈等,1994;王江海等,1998),认为大气成因地下水萃取地层中金属所形成的成矿流体(罗君烈等,1994;王江海等,1998;温春齐等,1995;胡瑞忠等,1998)上升到地表同生沉积成矿。新近有人提出成矿卤水在成岩过程中沿大断裂向上移动,矿质通过交代碳酸盐岩地层和断层附近的沉积物,沉淀成超大型矿床(Li,1998);惰性气体同位素和流体包裹体地球化学研究在金顶矿区成矿流体中发现地幔流体(Xue et al., 2000;薛春纪等,2002)。

在前人工作的基础上,笔者对金顶矿床进行了野外和室内研究。本文通过对矿床地质、同位素和地球化学研究,分析了金顶矿床的若干基本事实。

* 本文受国家重点基础研究发展规划项目(编号: G1999043201)、中国博士后科学基金项目和国家计委地质科学专门项目(编号: 地科专 98-01)联合资助

第一作者简介 薛春纪,男,1962 年生,教授,博士生导师,从事矿床学、资源勘查教学与研究工作。

收稿日期 2001-01-18;改回日期 2002-02-27。张绮玲编辑。

❶ 朱上庆,覃功炯,陈式房,等. 1995. 金顶超大型陆相碎屑岩铅锌矿床. 攀登项目(A30-04)专题研究报告.

1　矿区地质及演化

矿区地质演化中存在沉积作用、推覆活动、热隆升-金属成矿、穹隆破裂等基本地质事件，它们大致反映出从沉积作用→推覆活动→热隆升-大规模成矿→隆升持续-穹隆破裂的地质演化过程(图 1)。

矿区沉积了中—新生界。从新到老依次为第四系，第三系始新统果郎组(E_2g)岩屑石英砂岩，古新统云龙组上段(E_1y^b)角砾岩和砂岩、下段(E_1y^a)粉砂泥岩，中白垩统虎头寺组(K_2h)和下白垩统景星组(K_1j)石英砂岩及粉砂岩，中侏罗统花开左组(J_2h)粉砂岩和泥岩，上三叠统麦初箐组(T_3m)粉砂-细砂岩、挖鲁扒组(T_3w)泥岩和粉砂岩、三合洞组(T_3s)灰岩夹白云岩。矿体主要产在古新统云龙组上段和下白垩统景星组中。云龙组上段的岩性变化较大，矿区东部多为角砾岩、大岩块砂砾岩，向西变为砾质-含砾石英砂岩、细砂岩；该组地层具有

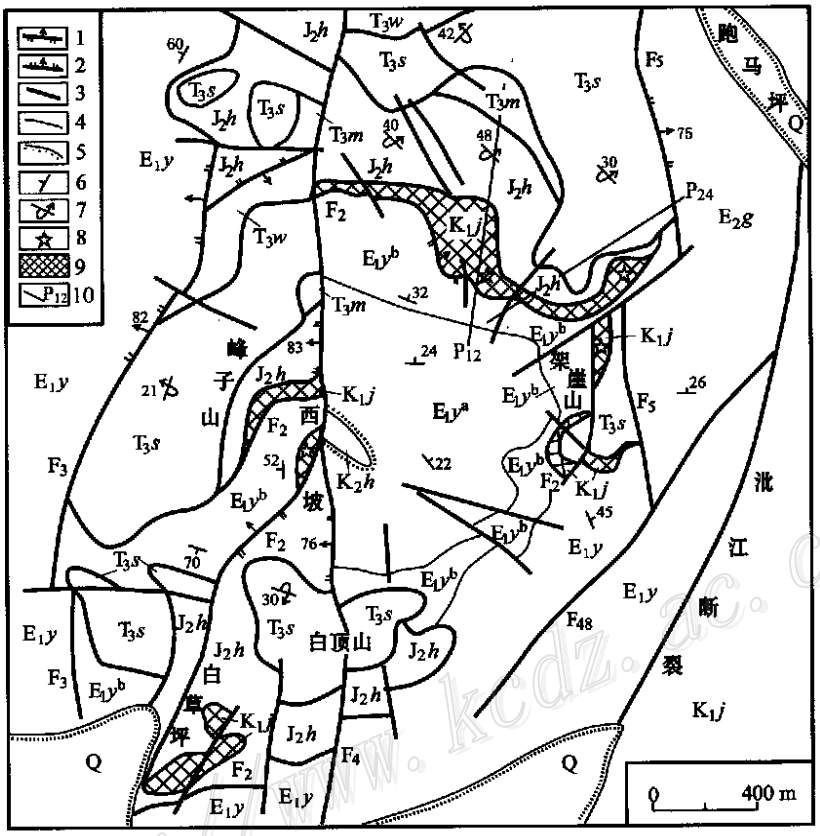

图 1　金顶铅锌矿区地质图(据云南地质第三大队 1989 年勘探报告)

Q—第四系；E_2g—始新统果郎组岩屑石英砂岩；E_1y—古新统云龙组；E_1y^b—云龙组上段角砾岩和砂岩；E_1y^a—云龙组下段粉砂泥岩；K_2h—中白垩统虎头寺组石英砂岩及粉砂岩；K_1j—下白垩统景星组粗砂岩和岩屑石英砂岩；J_2h—中侏罗统花开左组粉砂岩和泥岩；T_3m—上三叠统麦初箐组含膏盐粉砂-细砂岩；T_3w—上三叠统挖鲁扒组泥岩和粉砂岩；T_3s—上三叠统三合洞组灰岩夹白云岩；1—逆冲推覆断裂；2—正断层；3—性质不明断裂；4—地质界线；5—不整合面；6—正常岩层产状；7—倒转岩层产状；8—重点调研取样位置；9—铅锌矿体；10—勘探线及编号

Fig. 1　Geological map of the Jinding lead-zinc ore district (after the exploration report by No.3 geological party, Yunnan, 1989)

Q—Quaternary; E_2g—Debris quartz sandstone of Eocene Guolang Formation; E_1y—Paleocene Yunlong Formation; E_1y^b— Upper Member of Yunlong Formation: breccia and sandstone; E_1y^a—Lower Member of Yunlong Formation: siltstone and mudstone; K_2h—Middle Cretaceous Hutousi Formation: quartz sandstone and siltstone; K_1j—Lower Cretaceous Jingxing Formation: megagrained sandstone and debris quartz sandstone; J_2h—Middle Jurassic Huakaizuo Formation: siltstone and mudstone; T_3m—Upper Triassic Maichuqing Formation: salt-bearing siltstone and fine sandstone; T_3w^l—Upper Triassic Waluba Formation: mudstone and siltstone; T_3s—Upper Triassic Sanhedong Formation: limestone with dolomite; 1—Thrusting napped fault; 2—Normal fault; 3—Undeterminate fault; 4—Geological boundary; 5—Unconformity; 6—Attitude of normal stratum; 7—Attitude of reversed stratum; 8—Sample location; 9—Lead-zinc orebody; 10—Exploration line and serial number

活动性冲积扇沉积特征(覃功炯,1981),角砾是来自上三叠统三合洞组、麦初箐组及中侏罗统花开左组的灰岩、页岩和粉砂岩,岩层东厚西薄(图 2)。景星组主要为粗砂岩和岩屑石英砂岩细砂岩。受逆冲推覆构造影响,中—新生界彼此之间多以推覆构造面接触(图 2)。

金顶逆冲推覆构造是兰坪盆地古新世云龙期后区域大型推覆构造的组成部分,在矿区表现为以 F_2 逆冲推覆构造为主及与它平行的其它逆冲断层(图 1,图 2)。从矿区东部推覆而来的"外来系统"以 F_2 为界覆于矿区"原地系统"之上。原地系统为正常层序,由虎头寺组(K_2h)和云龙组(E_1y^a-E_1y^b)构成(图 1);外来系统地层倒转,从下到上依次为 K_1j、J_2h、T_3m 和 T_3s,各组岩层之间均分别以次级逆冲断层接触(图 2,图 3)。矿体为板状、脉状和透镜状产在推覆构造(F_2)中及其上下的景星组(K_1j)和云龙组上段(E_1y^b)碎屑岩中。推覆构造是一种容矿构造。逆冲推覆断层面连同主矿体在矿区东部东倾,北部北倾,西部西倾,南部南倾,形成以推覆构造原地系统为核心的穹隆构造(图 1);根据推覆滑动面也卷入到穹隆中可以判断推覆构造发生在穹隆构造之前(吴淦国等,1989)。

金顶穹隆构造地表出露范围 3 × 2.5(km^2),为一北北东向稍长的椭圆形,核部出露地层为中白垩统虎头寺组和古新统云龙组(原地系统),顶部及周边是推覆构造,为下白垩统、中侏罗统和上三叠统(外来系统),岩层和矿体围绕着穹隆核心分布,矿体厚度越靠近穹隆顶部越厚(图 1,图 3)。穹隆孤立出现,其北北东走向与区域北北西向主构造线方向不相协调,且卫星数字图象解译发现了反映深部岩浆等热源体客观存在的多级环形构造,在一定程度上指示了隐伏岩浆活动的状态(罗君烈等,1994;葛良胜等,1999;薛春纪等,2000),结合兰坪盆地内喜马拉雅期 25 ~ 30 Ma 幔源或壳幔源碱性岩体分布较多

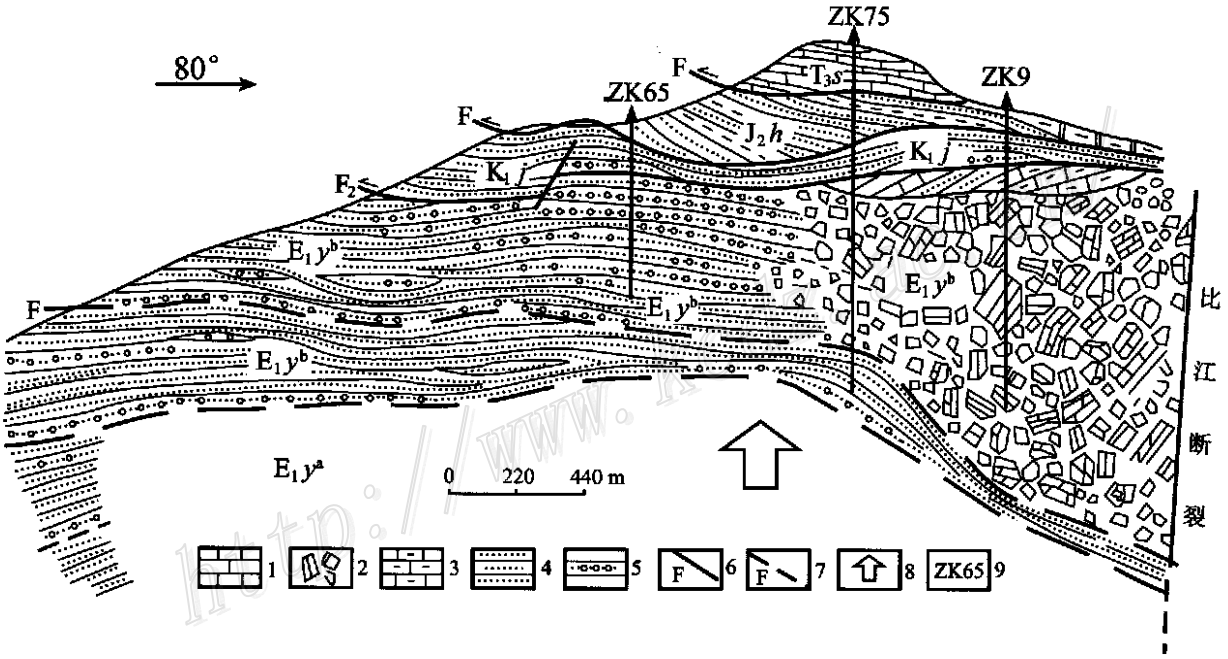

图 2 金顶矿区古新统云龙组上段(E_1y^b)岩相变化及逆冲推覆构造示意图(据施加辛等,1983 简化)

E_1y^b—古新统云龙组上段;E_1y^a—古新统云龙组下段;K_1j—下白垩统景星组;J_2h—中侏罗统花开左组;T_3s—上三叠统三合洞组;1—灰岩;2—角砾岩;3—泥灰岩;4—砂岩、粉砂岩;5—角砾以灰岩为主的角砾岩;6—逆冲推覆断层;7—推测逆断层;8—推覆活动末及以后的热隆升;9—钻孔编号

Fig. 2 Lithofacies variation of Paleocene upper Yunlong Formation (E_1y^b) and the thrusting nappe structure in Jinding orefield (simplified from Shi Jiaxin et al, 1983)

E_1y^b—Upper Member of Paleocene Yunlong Formation; E_1y^a—Lower Member of Paleocene Yunlong Formation; K_1j—Lower Cretaceous Jingxing Formation; J_2h—Middle Jurassic Huakaizuo Formation; T_3s—Upper Triassic Sanhedong Formation; 1—Limestone; 2—Breccia; 3—Marl; 4—Sandstone, siltstone; 5—Briccia with limestone rubble; 6—Thrusting napped fault; 7—Inferred thrusting fault; 8—Thermal doming after thrusting napped activity; 9—Drill number

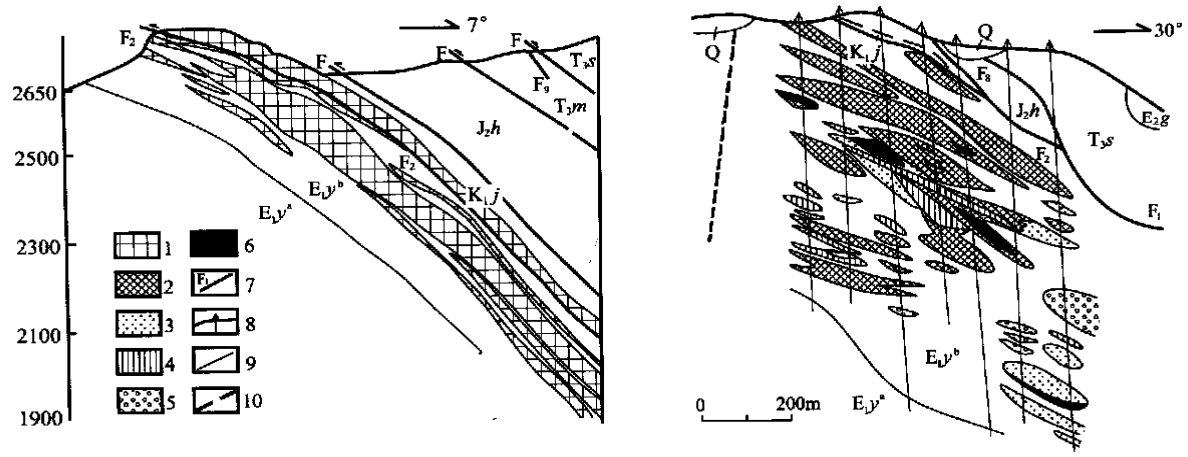

图 3　金顶铅锌矿床 12 勘探线(左)和 24 勘探线(右)剖面图(据云南地质三大队 1989 年勘探报告)

Q—第四系 ; E_2g—始新统果郎组 ; E_1y^b—古新统云龙组上段 ; E_1y^a—古新统云龙组下段 ; K_1j—下白垩统景星组 ; J_2h—中侏罗统花开左组 ; T_3m—上三叠统麦初箐组 ; T_3s—上三叠统三合洞组 ; 1—矿体(未分) ; 2—铅锌矿体 ; 3—天青石矿体 ; 4—硫铁矿体 ; 5—石膏矿体 ; 6—天青石铅锌矿体 ; 7—逆冲推覆断层及编号 ; 8—钻孔 ; 9—地层界线 ; 10—推测的正断层

Fig. 3　Sections along No.12 and No.24 exploration lines in the Jinding Pb-Zn ore deposit (After No.3 Geological Party, Yunnan Province, 1989)

Q—Quaternary ; E_1g—Eocene Guolang Formation ; E_1y^b—Upper Member of Paleocene Yunlong Formation ; E_1y^a—Lower Member of Paleocene Yunlong Formation ; K_1j—Lower Cretaceous Jingxing Formation ; J_2h—Middle Jurassic Huakaizuo Formation ; T_3m—Upper Triassic Maichuqing Formation ; T_3s—Upper Triassic Sanhedong Formation ; 1—Orebody (undivided) ; 2—Pb-Zn orebody ; 3—Celestite orebody ; 4—Pyrite orebody ; 5—Gypsum orebody ; 6—Celestite Pb-Zn orebody ; 7—Thrusting napped faults and their serial number ; 8—Drill hole ; 9—Stratigraphic boundary ; 10—Inferred normal fault

(云南地质矿产局,1990 ;尹汉辉等,1990 ;葛良胜等,1999 ;吕伯西等,1999),最近在碱性岩中发现幔源包体(吕伯西等,1999),喜马拉雅期热流变质(无量山变质带中绢云母 K-Ar 法年龄 24 ~ 31 Ma,云南地质矿产局,1990 ;范承钧等,1993 ;罗君烈等,1994 ;梅英,1998)也较发育,推测金顶穹隆为热隆升造成,可能与隐伏岩体或幔流上涌有关,铅锌成矿作用随热隆升的开始而发生。这种热穹隆和大规模成矿应发生在云龙组沉积和推覆活动以后,与第三纪碱性岩浆活动及热流变质作用开始的时间接近。

热穹隆和大规模铅锌矿体形成以后,矿区持续隆升,以穹隆核部为中心出现十几条放射状断裂,穹隆破裂,岩层和矿体显现出断续分布的特点(图 1)。

2　矿体、容矿岩石及成矿特征

金顶矿体为板状、脉状和透镜状,明显受推覆构造控制,主体产在逆冲断裂 F_2 及其上的景星组(上含矿带)和其下的云龙组上段顶部(下含矿带)陆相碎屑岩中(图 2,图 3),矿体产状与推覆构造及地层大体一致,而平面上铅锌矿体呈环形,断续围绕穹隆核心分布(图 1)。矿体厚度一般 0 ~ 40 m,靠近穹隆顶部最厚,可达 70 余米,反映推覆构造和热穹隆对成矿的双重控制,前者是成矿的空间准备,而后者是成矿的内在源动力,与成矿的时空关系更为密切。矿体的顶板(J_2h)和底板(E_1y^a 下段)均为细碎屑岩层,起到了隔挡层的作用。矿体与围岩界线不清楚,要靠样品圈定,没有 SEDEX 型矿床表现出的截然关系。I_1 号矿体产在景星组砂岩中,铅锌储量占整个矿床储量的 40 %,顶板为侏罗系红层。与矿体接触部位常有 0.5 ~ 1.0 m 宽的退色带(罗君烈等,1994),由红色碎屑岩的硅化所致,这种矿体顶板的热液蚀变在 SEDEX 型矿床中是不可能出现的。除铅锌矿体外,在矿区东部比江断裂附近的深部还有黄铁矿矿体、天青石矿体;除主矿体外,少部分铅锌矿体产于云龙组下段(E_1y^a)和中侏罗统花开左组(J_2h)中(罗君烈等,1994),说明成矿对构造和岩性而不是对层位有选择性。没有作为矿体容矿岩石或与之相伴的热水沉积岩。

为阐明成矿特征,首先对矿区及外围与上下矿

带处于同一层位的不含矿容矿岩石进行岩相学研究。作为上含矿带容矿主岩的石英砂岩中陆源碎屑成分主要是石英,其次为硅质岩屑,少量长石;作为下含矿带容矿主岩的角砾岩和砾质砂岩的陆源碎屑成分主要是灰岩、白云岩、页岩及粉砂岩岩块和石英,少量长石。岩块多棱角状,直径一般几到几百厘米,大者达几十到几百米。这些含矿主岩的胶结物为钙质及少量粘土质。矿石中天青石(少量重晶石)和硫化物(黄铁矿、闪锌矿、方铅矿、白铁矿)交代主岩中的钙质胶结物,硫化物交代原砂岩中钙质胶结物形成的胶结结构是最为典型的矿石结构。天青石、重晶石最早对碎屑岩中钙质胶结物交代,形成于热液成矿早阶段,与黄铁矿和少量闪锌矿共生,并被晚阶段硫化物交代。黄铁矿常有几个世代,早期的多微晶-胶状与天青石、闪锌矿、方铅矿共生,可被闪锌矿、方铅矿交代,晚期的多呈粗晶(脉),自形程度高,与方解石及粗晶方铅矿共生。热液成矿主阶段形成"闪锌矿 + 方铅矿 + 黄铁矿"典型共生组合,具有微晶-胶状结构,浸染状构造,未见层(纹)状矿石构造。这些现象说明金顶热液大规模铅锌成矿发生在碎屑沉积-成岩以后,没有同生沉积成矿的事实。

3 矿化分带

金顶矿床中元素和矿物具有明显分带现象(罗君烈等,1994),由矿区东部往西部,从深部到浅部,表现出 Sr + Ba → Fe → Zn + Pb → Pb,或天青石 + 重晶石 → 黄铁矿 + 白铁矿 → 闪锌矿 + 方铅矿 → 方铅矿(图 3 中右图)。金顶矿床具有与 SEDEX 型矿床不同的分带规律(图 4),说明金顶铅锌矿床具有不同于 SEDEX 的成矿机制。SEDEX 型成矿过程中因氧化还原电位变化而导致金属沉积物随离开热液喷口远近不同出现矿物分带的现象,在金顶矿床中并未表现,这种分带可能与热液流体矿化的阶段性相联系。

4 铅、硫同位素及成矿温度与深度

前人(赵兴元,1989;周维全等,1992;叶庆同等,1992;张乾,1993;罗君烈等,1994)已经积累了金顶矿床的大量硫化物的 Pb、S 同位素数据。通过对 96 件 Pb 同位素数据统一求算模式年龄和源区特征值,发现有 85 %的样品反映幔源 Pb 特征(模式年龄主频

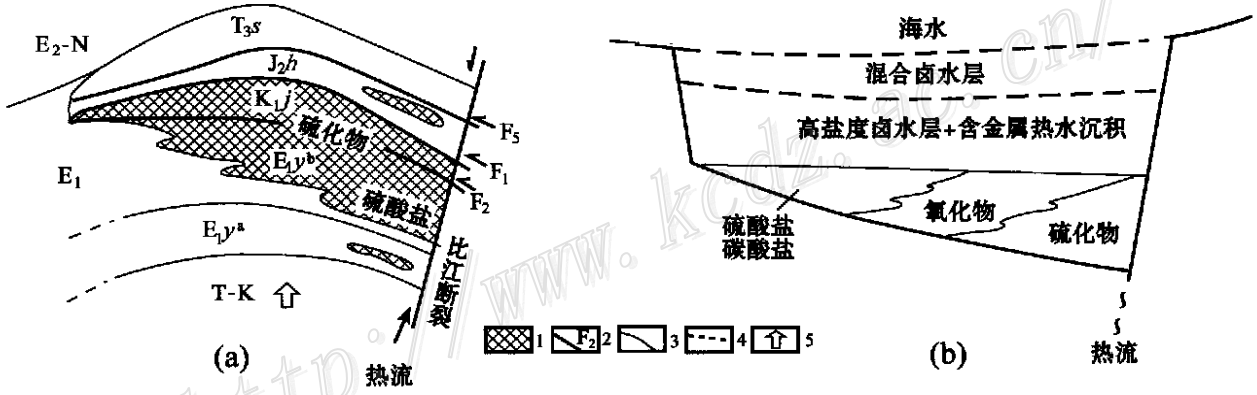

图 4 金顶铅锌矿床理想矿化分带(a)及与 SEDEX 型矿床(b)的对比

(a 图据罗君烈等,1994 资料编绘;b 图据 R. W. Hutchinson,1988)

E_2-N—始新统-上新统;E_1—古新统;E_1y^b—古新统云龙组上段;E_1y^a—古新统云龙组下段;K_1j—下白垩统景星组;J_2h—中侏罗统花开左组;T_3s—上三叠统三合洞组;T-K—三叠系-白垩系;1—矿体及矿化体;2—逆冲推覆断裂;3—地层界线;4—水体分层界线;5—推覆活动末及以后的热隆升

Fig. 4 Comparison of the theoretical mineralizing zonality in the Jinding Pb-Zn deposit (a) with that in the exhalation sedimentary deposit (b)

E_2-N—Eocene-Pleocene; E_1—Paleocene; E_1y^b—Upper Member of Paleocene Yunlong Formation; E_1y^a—Lower Member of Paleocene Yunlong Formation; K_1j—Lower Cretaceous Jingxing Formation; J_2h—Middle Jurassic Huakaizuo Formation; T_3s—Upper Triassic Sanhedong Formation; T-k—Triassic-Cretaceous; 1—Ore and ore-bearing body; 2—Thrusting napped faults; 3—Stratigraphic boundary; 4—Layer boundary of water body; 5—Thermal doming after the thrusting nappped activity

位于 42 Ma ,μ 值主频在 8 .87) ,其余 15 %显示壳幔混合铅特征(模式年龄主频位于 102 Ma ,μ 值主频在 9 .05) 。对文献中 88 件硫化物矿物样品 S 同位素数据的统计表明 ,$\delta^{34}S$ 出现 3 个峰值 : - 4 .5 ‰(黄铁矿样品占 78 .9 %) 、- 13 .5 ‰(闪锌矿样品占 81 %) 和 - 19 .0 ‰(方铅矿样品占 87 .1 %) (图 5) , 存在 $\delta^{34}S_{黄铁矿} > \delta^{34}S_{闪锌矿} > \delta^{34}S_{方铅矿}$ 的趋势 , 说明成矿流体中硫化物之间相互平衡 , 总体上富轻硫的特征反映还原硫与地层中大量硫酸盐的还原作用有关 。

金顶铅锌矿石中石英 、天青石 、闪锌矿 、方解石 、石膏等矿物流体包裹体均一温度在 52 ~ 309 ℃间(叶庆同等 ,1992 ; 罗君烈等 ,1994 ; 温春齐等 ,1995) , 具中低温特点 ;188 个测温数据的统计显示 3 个温度区间 , 即 240 ~ 160 ℃ 、150 ~ 110 ℃和 100 ~ 50 ℃ , 其中 150 ~ 110 ℃的区间最为突出(图 5) , 它们可能分别代表了热液成矿 3 个阶段的温度 。成矿压力估计为 32 .5 ~ 22 .6 MPa , 成矿深度相当于 1 .46 ~ 0 .91 km (温春齐等 ,1995) , 此深度不应与上覆水体的静压力对应 , 而应为上覆岩层的厚度 , 因为成矿主岩是陆相碎屑沉积的冲积扇相(覃功炯 ,1981) 。1 .46 ~ 0 .91 km 的成矿深度与 SEDEX 型和 SST 矿床显然不同 。

成矿流体的盐度 $w(NaCl_{eq})$ 为 5 .09 % ~ 19 .63 % , 多为 7 .5 %左右 , 属中低盐度(叶庆同等 , 1992 ; 罗君烈等 ,1994 ; 温春齐等 ,1995) ; 如果成矿流体纯粹起源于盆地中 —新生代地层中的大气成因地下水 , 则如此之低的流体盐度是难以理解的 , 因为兰坪蒸发盆地中-新生界内发育多个含膏盐层位 。

5　结　论

金顶铅锌矿床有别于其他地区以沉积岩为主岩的铅锌矿床 , 其明显特色如下 :

矿区大致先后经历了沉积作用 、推覆活动 、热隆升-流体成矿和隆升持续-穹隆破裂 4 个地质演化阶段 , 成矿作用是伴随推覆挤压应力释放以后出现的局部引张隆升-热流活动而发生的 , 成矿时间与该区喜马拉雅期强烈碱性岩浆活动和热流变质开始的时间接近 。

矿体呈板状 、脉状产在中新生界陆相碎屑岩中 , 受构造和高孔隙岩性控制明显 , 没有出现确切的同生沉积成矿事实和在 SEDEX 型矿床中伴随出现的的热水沉积岩 。典型的矿石结构是热液硫化物矿物交代高孔渗碎屑岩中胶结物形成的胶结结构 , 微晶-胶状未见层纹状矿石构造 。

内生流体成矿分为 3 个阶段 , 矿化分带及成矿作用与 SEDEX 型矿床不同 。

成矿温度中等 , 成矿深度 0 .9 ~1 .5 km , 成矿流体盐度中等偏低 。硫化物铅同位素组成主体反映地幔铅 , 硫化物富轻硫 。

致　谢　感谢几次野外工作中给予指导 、帮助和大力支持的云南地矿局罗君烈和丁俊总工程师 ; 对涂光炽院士 、覃功炯教授 、金景福教授及刘建明研究员在研究工作中给予的启发表示敬意和谢忱 !

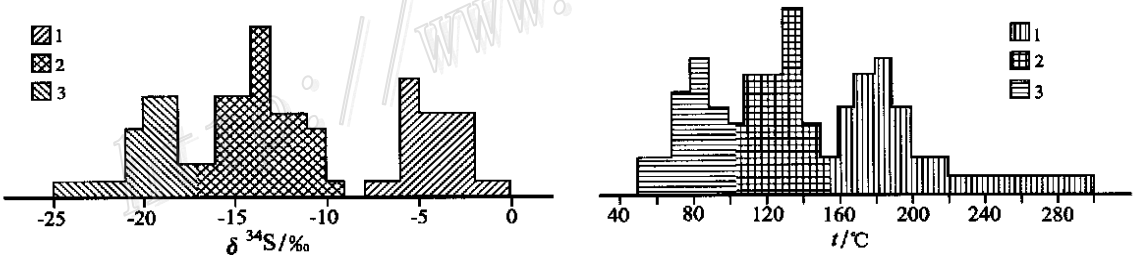

图 5　金顶铅锌矿床 $\delta^{34}S$ 和流体包裹体均一温度直方图

(据赵兴元 ,1989 ; 周维全等 ,1992 ; 叶庆同等 ,1992 ; 张乾 ,1993 ; 罗君烈等 ,1994 ; 温春齐等 ,1995 资料统计绘制)

左图 :1 —黄铁矿样品占该区间 78 .9 % ; 2 —闪锌矿样品占该区间 81 % ; 3 —方铅矿样品占该区间 87 .1 % ; 右图 : 1 —石英 、天青石样品占该区间 84 % ; 2 —天青石 、闪锌矿样品占该区间 77 % ; 3 —方解石 、石膏样品占该区间 82 %

Fig . 5　$\delta^{34}S$ and homogenization temperature histogram of inclusions in the Jinding Pb-Zn deposit

(after Zhao , 1989 ; Zhou et al . , 1992 ; Ye et al . , 1992 ; Zhang , 1993 ; Luo et al . , 1994 ; Wen et al . , 1995)

The left : 1 —Pyrite samples occupy 78 .9 % of the area ; 2 —Sphanerite samples occupy 81 % of the area ; 3 —Galena samples account for 87 .1 % of the area . The right : 1 —Quartz and celestite samples make up 84 % of the area ; 2 —Celestite and sphanerite samples account for 77 % of the area ; 3 —Calcite and gypsum samples occupy 82 % of the area

References

Bai J F, Wang C H and Na R X. 1985. Geological characteristics of the Jinding lead-zinc deposit in Yunnan with a special discussion on its genesis[J]. Mineral Deposits, 4(1): 1 ~ 9 (in Chinese with English abstract).

Fan C J and Zhang Y F. 1993. Geological-tectonic pattern in weastern Yunnan[J]. Yunnan Geology, 12(2): 101 ~ 110 (in Chinese with English abstract).

Gao G L. 1989. Review of geological origin about Jinding lead-zinc ore deposit[J]. Earth Science. 14(5): 467 ~ 475 (in Chinese with English abstract).

Ge L S, Yang J H, Guo X D, et al. 1999. The hidden E W-structure existing in north-western Yunnan and the evidence[J]. Yunnan Geology, 18(2): 155 ~ 167 (in Chinese with English abstract).

Hu M A. 1989. A preliminary evaluation of the mineralization and their characteristics on the karst-type lead-zinc deposit by the exemplification of Jinding, Yunnan province[J]. Earth Science, 14(5): 531 ~ 538 (in Chinese with English abstract).

Hu R Z, Zhong H, Ye Z J, et al. 1998. Helium and argon isotope geochemistry of Jinding large-scale lead-zinc deposit [J]. Science in China (D series), 28(3): 208 ~ 213.

Hutchinson R W. 1988. The new advances of stratabound deposit researches[J]. Mineral Deposits Abroad, (3): 2 ~ 82 (in Chinese).

Jue M Y, Cheng D M, Zhang L S, et al. 1998. Copper deposits in Lanping-Simao Basin [M]. Beijing: Geological Publishing Huose. 1 ~ 17, 37 ~ 46 (in Chinese).

Li N. 1998. Depositional controls and genesis of the Jinding sandstone-hosted Zn-Pb deposit, Yunnan province, Southwest China[D]. (for the degree of Ph. D). The University of Texas at Austin. U.S.A.

Luo J L and Yang J Z. 1994. Tethyan evolution and the mineralization of the main metal deposits in western Yunnan [M]. Beijing: Geological Publishing Huose. 149 ~ 239 (in Chinese).

Lu B X and Qian X G. 1999. Petrology research on the deep source inclusions of alkali volcanic rock and alkali-rich porphyry in the Cenozoic Era at western Yunnan[J]. Yunnan Geology, 18(2): 127 ~ 143 (in Chinese with English abstract).

Qin G J. 1981. An idea about Jinding structure active alluvial fan[J]. Geological Research, (1): 11 ~ 26 (in Chinese with English abstract).

Qin G J and Zhu S Q. 1991. The ore-forming model of Jinding lead-zinc deposit and ore deposits forecast[J]. Yunnan Geology, 10(2): 145 ~ 190 (in Chinese with English abstract).

Shi J X, Yi F H, Wen Q D, et al. 1983. The rock-ore characteristics and mineralization of Jinding lead-zinc deposit, Lanping [J]. Yunnan Geology, 2(3): 179 ~ 195 (in Chinese with English abstract).

Wang J H, Yan W, Chang X Y, et al. 1998. Continental hydrothermal sedimentation: A Case Study of the Yunnan area, China [M]. Beijing: Geological Publishing House. 79 ~ 89 (in Chinese).

Wang J B and Li C Y. 1991. REE geochemistry of the Jinding super-large Pb-Zn deposit [J]. Geochimica, 19(4): 359 ~ 365 (in Chinese with English abstract).

Wen C Q, Cai J M, Liu W Z, et al. 1995. The geochemical characteristics of the fluid inclusion in Jinding lead-zinc deposit, Yunnan, China [J]. J. Mineral Petrol., 15(4): 78 ~ 84 (in Chinese with English abstract).

Wu G G and Wu X D. 1989. A preliminary study on the tectonic evolution and mineralization regularity of the Jinding lead-zinc deposit, Yunnan province[J]. Earth Science, 14(5): 477 ~ 486 (in Chinese with English abstract).

Xue C J, Wang D H, Chen Y C, et al. 2000. Helium, argon, and xenon isotopic compositions of ore-forming fluids in Jinding-Baiyangping polymetallic deposits, Yunnan, Southwest China[J]. Acta Geologica Sinica, 74(3): 521 ~ 528 (in Chinese with English abstract).

Xue C J, Chen Y H, Wang D H, et al. 2002. The CO_2-rich and hydrocarbon-bearing ore-forming fluid and their metallogenic role in the Lanping Pb-Zn-Ag-Cu orefield, north-western Yunnan[J]. Acta Geologica Sinica, 76(2): 102 ~ 116.

Ye Q T, Hu Yu Z and Yang Y Q. 1992. Regional geochemistry background and the gold-silver-lead-zinc mineralization in Sanjiang area [M]. Beijing: Geological Publishing Huose. 217 ~ 264 (in Chinese).

Yin H H, Fan W M and Lin Ge. 1990. Deep factors on the Lanping-Simao basin evolution and the mantle-crust complex mineralizations [J]. Tectonic and Metallogeny, 4(2): 113 ~ 124 (in Chinese with English abstract).

Yunnan Geological and Mineral Resources Bureau. 1990. Annals of Regional Geology, Yunnan Province[M]. Beijing: Geological Publishing Huose. 106 ~ 278 (in Chinese with English abstract).

Zhang Q. 1993. Pb isotopic composition of Jinding super-large Pb-Zn in Yunnan province and Discussion on the sources of lead[J]. Geology and Prospecting, 29(5): 21 ~ 28 (in Chinese with English abstract).

Zhao X Y. 1989. On the genesis of the Jinding lead-zinc ore deposit in Yunnan[J]. Earth Science, 14(5): 523 ~ 530 (in Chinese with English abstract).

Zhou W Q and Zhou Q L. 1992. A study on the isotopic composition of Pb and S in the Lanping Pb-Zn deposit, Yunnan Province [J]. Geochimica, 20(2): 141 ~ 148 (in Chinese with English abstract).

附中文参考文献

白嘉芬, 王长怀, 纳荣仙. 1985. 云南金顶铅锌矿床地质特征及成因初探[J]. 矿床地质, 4(1): 1 ~ 9.

范承钧, 张翼飞. 1993. 云南西部地质构造格局[J]. 云南地质, 12(2): 101 ~ 110.

高广立. 1989. 论金顶铅锌矿床的地质问题[J]. 地球科学, 14(5): 467 ~ 475.

葛良胜, 杨嘉禾, 郭晓东, 等. 1999. 滇西北地区(近)东西向隐伏构造带的存在及证据[J]. 云南地质, 18(2): 155 ~ 167.

胡明安. 1989. 试论岩溶型铅锌矿床的成矿作用及其特点——以云

南金顶矿床为例[J]. 地球科学, 14(5): 531 ~ 538.
胡瑞忠, 钟　宏, 叶造军, 等. 1998. 金顶超大型铅-锌矿床氦、氩同位素地球化学[J]. 中国科学(D辑), 28(3): 208 ~ 213.
阚梅英, 程敦摸, 张立生, 等. 1998. 兰坪-思茅盆地铜矿床[M]. 北京: 地质出版社. 1 ~ 17, 37 ~ 46.
Hutchinson R W. 1988. 层控矿床在地质历史中的地位[J]. 国外矿床地质, (3): 2 ~ 82.
罗军烈, 杨荆舟. 1994. 滇西特提斯的演化及主要金属矿床成矿作用[M]. 北京: 地质出版社. 149 ~ 239.
吕伯西, 钱祥贵. 1999. 滇西新生代碱性火山岩、富碱斑岩深源包体岩石学研究[J]. 云南地质, 18(2): 127 ~ 143.
覃功炯. 1981. 关于金顶构造活动型冲积扇的认识[J]. 地学研究, (1): 11 ~ 26.
覃功炯, 朱上庆. 1991. 金顶铅锌矿床成因模式及找矿预测[J]. 云南地质, 10(2): 145 ~ 190.
施加辛, 易凤煌, 文　其. 1983. 兰坪金顶铅锌矿床的岩矿特征及成因[J]. 云南地质, 2(3): 179 ~ 195.
王江海, 颜　文, 常向阳, 等. 1998. 陆相热水沉积作用-以云南地区为例[M]. 北京:地质出版社. 79 ~ 89.
王京彬, 李朝阳. 1991. 金顶超大型铅锌矿床 REE 地球化学研究[J]. 地球化学, 19(4): 359 ~ 365.
温春齐, 蔡建明, 刘文周, 等. 1995. 金顶潜锌矿床流体包裹体地球化学特征[J]. 矿物岩石, 15(4): 78 ~ 84.
吴淦国, 吴习东. 1989. 云南金顶铅锌矿床构造演化及矿化富集规律[J]. 地球科学, 14(5): 477 ~ 486.
薛春纪, 陈毓川, 王登红, 等. 2002. 滇西北兰坪铅锌银铜矿田含烃富 CO_2 成矿流体及其地质意义[J]. 地质学报, 76(2): 102 ~ 116.
叶庆同, 胡云中, 杨岳清. 1992. 三江地区区域地球化学背景和金银铅锌成矿作用[M]. 北京: 地质出版社. 217 ~ 246.
尹汉辉, 范蔚茗, 林　舸. 1990. 云南兰坪-思茅地洼盆地演化的深部因素及幔-壳复合成矿作用[J]. 大地构造与成矿学, 4(2): 113 ~ 124.
云南省地质矿产局. 1990. 云南省区域地质志[M]. 北京: 地质出版社. 106 ~ 278.
张　乾. 1993. 云南金顶超大型铅锌矿床的铅同位素组成及铅来源探讨[J]. 地质与勘探, 29(5): 21 ~ 28.
赵兴元. 1989. 云南金顶铅锌矿床成因研究[J]. 地球科学, 14(5): 523 ~ 530.
周维全, 周全立. 1992. 兰坪铅锌矿床铅和硫同位素组成研究[J]. 地球化学, 20(2): 141 ~ 148.

Jinding Pb-Zn Deposit: Geology and Geochemistry

Xue Chunji[1], Chen Yuchuan[2], Yang Jianmin[3], Wang Denghong[3], Yang Weiguang[4] and Yang Qingbiao[4]

(1 Open Research Laboratory of Mineralization and Its Dynamics, MLR; Department of Geology and Mineral Resources, Chang'an University, Xi'an 710054, Shaanxi, China; 2 Chinese Academy of Geological Sciences, Beijing 100037, China; 3 Institute of Mineral Resources, Chinese Academy of Geological Sciences, Beijing 100037, China; 4 No.3 Geological Party of Yunnan Province, Dali 671000, Yunnan, China)

Abstract

Located in Lanping County, Yunnan Province, the Jinding Pb-Zn deposit is the largest polymetallic deposit in China. The orebodies are hosted in Mesozoic-Cenozoic terrestrial clastic rocks. No igneous rocks have ever been found in the orefield. The deposit has some unique features, which can distinguish it from such sedimentary rock-hosted deposits as MVT-type and Sedex type Pb-Zn deposits. The tabular orebodies (with some veins) are hosted in the Eocene Yunlong Formation and Lower-Cretaceous Jingxing Formation, both of which consist mainly of terrestrial clastic rocks. This leads to the syngenetic model proposed by some authors. The mineralization, however, is not lithostratigraphically restricted. Instead, it is controlled by faulting and doming. The major feeder fault is F_2, a thrust that had been formed at an earlier stage but was modified during the later doming. The orebodies occur in both hanging wall and foot wall. This, together with the absence of hydrothermal sediments and the ore textures of replacement and space-filling, suggests an epigenetic, hydrothermal origin. The Pb isotope data show that the metal is mainly derived from the mantle, mixed with less amounts of crustal lead. The S isotope data show a trend of $\delta^{34}S_{pyrite} > \delta^{34}S_{sphalerite} > \delta^{34}S_{galena}$, indicating an equilibrium between the minerals, and the sulphur is mainly of crustal source. The study of fluid inclusions in sphalerite and in associated

(下转第 245 页)(to be continued on p.245)

phosed marine facies sodic volcanic rocks in Zhangbaling area. Generally, three stages of quartz veins can be recognized, i.e., gold-deficient sulfide quartz veins, gold-rich quartz sulfide veins and gold-deficient barite and/or carbonate veins. The $^{40}Ar/^{39}Ar$ step-heating plateau ages of the late first-stage and the second-stage quartz aggregates from the Zhuding, Maoshan and Shangcheng gold deposits range between 116.1 ~ 0.6 Ma and 118.3 ~ 0.5 Ma and are quite close to their least apparent ages and isochronal ages respectively. All plateau, least apparent and isochronal ages range from 113.4 ~ 0.4 Ma to 118.3 ~ 0.5 Ma, considered to be the formation age range of the quartz. It is reasonable and reliable to take the $^{40}Ar/^{39}Ar$ age range of the quartz as the formation age range of gold-bearing quartz veins on the basis of spatial relationship between gold-bearing quartz veins and their country rocks. The gold deposits in the two areas were formed in Aptian Stage of Cretaceous, when the Ta-Lu fault zone moved as a normal fault with slightly right-lateral strike-skip, extended and had very strong magmatic activity. It is shown that the magmatic hydrothermal fluid is a very important component part in the ore-forming hydrothermal fluid in Fengyang and Zhangbaling areas. The gold ore deposits in Fengyang and Zhangbaling areas genetically related to the extensional movement of the Ta-Lu fault zone and the magmatic activity were formed under the extensional dynamic condition in Late Cretaceous. Therefore, the extensional movement of the Ta-Lu fault zone provided energy and space for magmatic and gold ore-forming processes.

Key words: formation age, quartz, $^{40}Ar/^{39}Ar$, gold deposit, Anhui

---

(上接第 263 页)(Continued from p.263)

and granite (0.21 and 0.26 respectively) indicate the efficiency of transfer of thermal energy to mechanical (explosive) energy from the interaction of hot magma with cold water is higher than 90 %. This serves as geochemical evidence for magma-exotic water mixing model of cryptoexplosive breccia. The $\delta^{34}S$ of ore-stage sulfide and $\delta^{31}C$ of ore-stage calcite show that the S and C are derived from the deep source, whereas the post-ore $\delta^{34}S$ and $\delta^{31}C$ are possessed of mixing source. These Pb isotopes of country rock (volcanic rock) and basement rock (granite and metamorphic rock) belong to anomalous Pb enriched in radioactive lead and constitute a linear array with Pb isotopes of K-feldspar, pyrite and galena. This implies that the ore-forming material (uranium) is characterized by multisource from host rock and basement rock.

Key words: stable isotope, water/rock ratio, magma-exotic water mixing explosive model, cryptoexplosive breccia, uranium deposit

---

(上接第 277 页)(Continued from p.277)

gangue minerals (quarts, celestine, calcite and gypsum) shows that the homogenization temperatures range from 52 ℃ to 309 ℃, clustered around 110 ~ 150 ℃, with salinities of 5.09 % ~ 19.63 % wt NaCl equivalent. The pressure was 32.5 ~ 22.6 MPa, corresponding to an ore-forming depth of 0.9 ~ 1.5 km.

Key words: stratigraphical and structural control, Pb and S isotope, homogenization temperature, salinity, Jinding Pb-Zn deposit